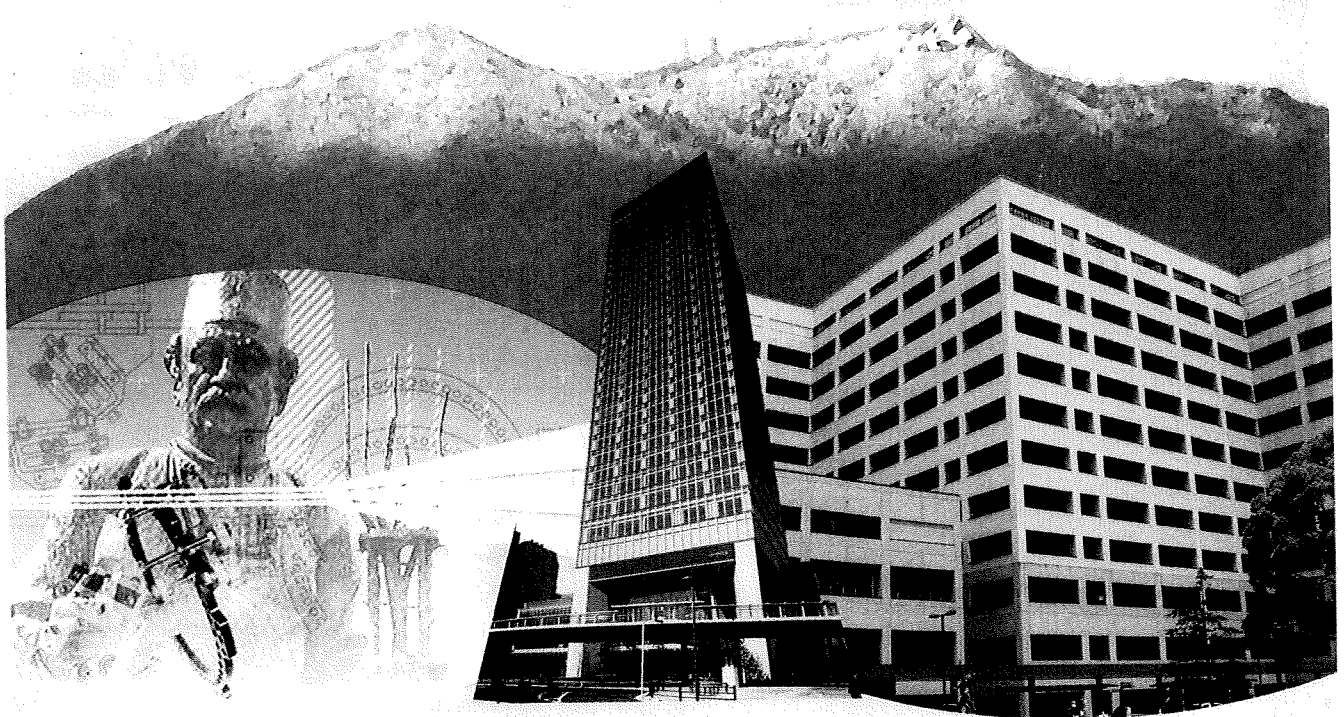


第23回

The 23rd Annual Meeting of Japanese Association of
External Fixation and Limb Lengthening

日本創外固定・骨延長学会

プログラム・抄録集

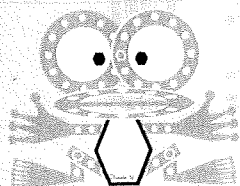


会期 2010.1/15(金)-1/16(土)

会場 秋葉原コンベンションホール

会長 落合 直之

筑波大学大学院人間総合科学研究科教授



Annual Meeting of
JAEFLL 2010

2-02**創外固定を用いたウサギ脛骨骨切りモデルにおける低出力超音波パルスの効果—マイクロCTを用いた3次元の Bone Strength Indices 評価—**

○飛田 健治、大西 五三男、松本 卓也、大橋 暁、別所 雅彦、金子 雅子、
中村 耕三

東京大学整形外科

Effect of low-intensity pulsed ultrasound stimulation on gap healing in a rabbit osteotomy model with external fixation evaluated by micro computed tomography-based 3-dimensional Bone Strength Indices

○Kenji Tobita, Isao Ohnishi, Takuya Matsumoto, Satoru Ohashi, Masahiko Bessho,
Masako Kaneko, Kozo Nakamura

Dept. of Orthop. Surg., Fac. of Med., Univ. of Tokyo

【背景】 低出力超音波パルス（以下LIPUS）治療の骨癒合への促進効果は臨床・基礎研究から実証されている。マイクロCT（以下 μ CT）は硬組織試料の非侵襲的3次元形態評価ができ、骨折治癒過程の精確な評価が可能である。Bone Strength Indices (BSI's)を用いた先行研究による骨強度評価は2次元評価であり、3次元（3D）的に評価したものは無い。

【目的】 創外固定を用いたウサギ脛骨骨切りモデルにおける低出力超音波パルスの効果を μ CTを用いて評価する。

【材料と方法】 21-23週齢、体重約4kgで雄の日本白色家兎42羽を用いた。吸入麻酔下右脛骨の骨切りを行い、2mmのGapを作成し両側式の創外固定を行った。LIPUSの照射/非照射群に分け、観察期間を4,6および8週とした。術後3日より1週間に6日、吸入麻酔下に20分間照射し、非照射群は照射群と同様の条件でダミーの振動子を用いて模擬照射を行った。観察終了後と殺し、 μ CT撮影を行った。関心領域はgapの中心1mmとし、XYZ空間上に設置した。X,Y及びZ軸周りのBSI'sを求めそれぞれ評価した。統計にはa one-way ANOVA testを行い、有意水準は $p < 0.05$ とした

【結果】 照射群は非照射群と比べ6週以降のBSI'sはX,Y及びZ軸すべての方向で有意に高値であった。4,6及び8週の非照射群間の比較では、BSI'sに有意差はなかった。また、4,6及び8週の照射群間の比較は3群間のBSI'sに有意差はなかった。

【考察】 BSI'sは慣性モーメントである。Ferretti等によって力学試験による実測値とCT断面像による2次元のBSI'sとの相関関係は立証されている。今回、3次元評価を行いLIPUS照射は捻じれ強度、曲げ強度を骨癒合過程早期に回復させることが示唆された。しかし、その後の骨強度回復に関しては不明である。

第83巻

第8号

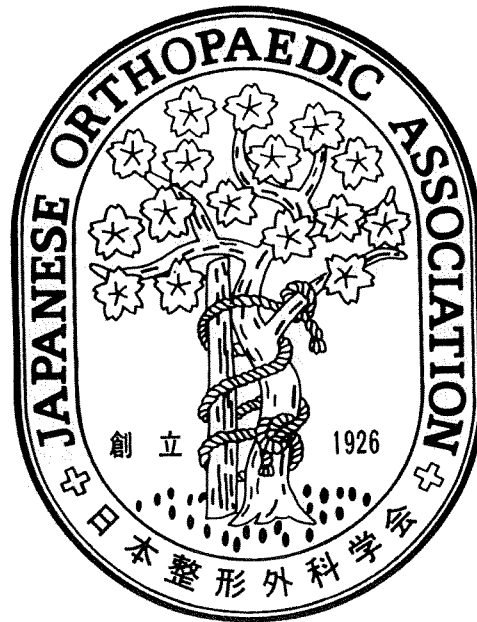
日本整形外科学會雜誌

NIPPON SEIKEIGEKAGAKKAI ZASSHI

The Journal of
the Japanese Orthopaedic Association

Vol. 83 No. 8 August 2009

Proceedings of the 24th Annual Research Meeting
of the Japanese Orthopaedic Association



日整会誌

社団法人 日本整形外科学会

J. Jpn. Orthop. Assoc.

2-E-5

GFP reporter を用いたマウス骨折治癒過程における woven bone 形成の評価

牛久 智加良¹ Douglas J. Adams²
David W. Rowe³ 斎藤 充¹ 丸毛 啓史¹

【目的】われわれはこれまでに、ラット1型コラーゲン(Col3.6)およびヒトオステオカルシン(hOC)プロモーター領域を使い、骨芽細胞の分化段階に応じてGFP(Green fluorescence protein)が発現するDual Transgenic(Tg)マウスを作製し、石灰化過程における細胞分化と基質合成の関係について報告してきた。今回、骨折治癒における仮骨の石灰化過程について同モデルを用いて解析したので報告する。

【方法】Col3.6GFPcyan, hOCGFPtpz dual Tg マウス(8週齢)の脛骨に閉鎖式骨折を作製した。骨折後7, 10, 14と30日目に脛骨を回収し蛍光顕微鏡を用いてGFPの発現を観察した。また屠殺前にXylenol orange(XO)を投与し、石灰化評価とHEおよびSafranin O染色による組織学的評価も行った。

【結果】骨折後7日目になると、仮骨部にCol3.6陽性細胞(Col3.6+)に囲まれたXO陽性の膜性骨化によるwoven bone(w/b)を認めた。10日目には、その表面に多くのCol3.6-hOC両陽性細胞が観察され、w/bはその厚みを増していた。14日目までに軟骨は内軟骨性骨化によるw/bに置換された。この時、仮骨中心部のw/bは主にCol3.6+に囲まれていたのに対し、骨折部、new cortical shellでは主にCol3.6-hOC両陽性細胞に囲まれていた。30日目には、仮骨中心部のw/bは骨髄様組織に置換されたが、骨折部、new cortical shellではその厚みを増していた。

【考察】これまで仮骨石灰化過程は、w/b形成を放射線、組織学的に観察することで評価されてきた。しかしその過程をGFP dual Tgマウスを用いて観察すると、hOC陽性細胞に囲まれたw/bが仮骨部に残存するのに対し、Col3.6陽性細胞に囲まれたw/bは早期に骨髄様組織に置換されることが明らかとなった。GFPトランスジェニックマウスを用いた骨折モデルでは、分化度の異なる細胞が仮骨石灰化過程に及ぼす影響を時間的に空間的に解析することが可能である。今後、骨折治癒過程に及ぼす薬剤や力学刺激などの影響を評価するモデルとして有用と考えられる。

¹慈恵医大整形 ²Dept. of Orthop. Surg., School of Medicine, Univ. of Connecticut Health Center, Farmington, CT, USA

³Dept. of Reconstructive Sciences, School of Dental Medicine, Univ. of Connecticut Health Center, Farmington, CT, USA

2-E-6

低出力超音波パルス治療の骨癒合リモデリング期に対する効果 —マイクロCTを用いた仮骨の髄腔化・皮質骨化の定量評価—

飛田 健治 大西 五三男 松本 卓也 大橋 暁
別所 雅彦 松山 順太郎 金子 雅子 中村 耕三

【背景】低出力超音波パルス(以下LIPUS)治療の骨癒合への促進効果は臨床・基礎研究から実証されている。マイクロCT(以下 μ CT)は硬組織試料の非侵襲的三次元形態評価ができ、骨折治癒過程の精確な評価が可能である。骨折のリモデリング期は仮骨の皮質骨化と共に髄腔化が起こり、骨癒合強度の回復に非常に重要であるが、これらを μ CTを用いて三次元的に定量評価した先行研究はない。

【目的】LIPUS照射がリモデリング期の仮骨に及ぼす効果を μ CTを用いて評価する。

【材料と方法】21-23週齢、体重約4kgで雄の日本白色家兎を用いた。吸入麻酔下右脛骨の骨切りを行い、2mmのgapを作成し両側式の創外固定を行った。LIPUSの照射/非照射群に分け、観察期間を4および8週とした。LIPUS照射は、術後3日より1週間に6日、吸入麻酔下に20分間行い、非照射群は照射群と同様の条件でダミーの振動子を用いて模擬照射を行った。観察終了後と殺し、仮骨の μ CT撮データを、骨量ファントムで定量化し評価した。対象部位はgapの中心1mmとし200 mg/cm³で2値化した仮骨をendosteal(以下E), intercortical (I), periosteal region (P)の3領域に分け、各領域におけるbone volume(以下BV), bone mineral content(以下BMC), BMC/BVの計測と、三次元的な二次モーメント、慣性モーメントとStress-Strain Index(以下SSI)から骨癒合強度予測を行った。LIPUS照射/非照射群の差の検定にはt検定を行った(有意水準<0.05)。

【結果】4週ではすべての評価項目で有意差が見られなかったが、8週において、LIPUS照射群は非照射群に対してBMC/BVはE, I, P共に有意に高値、BMCはEでは低下しており、I, Pで有意に高値、BVはIで有意に高値であった。また8週では二次モーメント、慣性モーメント、SSI共に有意に高値であった。

【考察】 μ CTを用いて、リモデリング期の仮骨髄腔化・皮質骨化に着目し定量評価した先行研究はない。今回の結果からLIPUSは仮骨の髄腔化・皮質骨化を促進した。またモーメント、SSIの増加からLIPUSは骨強度をより増加させることが示唆された。

東大大学院整形

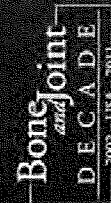
New Orleans 2010

56th Annual Meeting
of the Orthopaedic Research Society

March 6 - 9, 2010 • New Orleans, LA



Transactions



Abstracts

Program

Copyright

Help

Effect of low-intensity pulsed ultrasound stimulation on gap healing in a rabbit osteotomy model evaluated by micro computed tomography-based 3-dimensional cross-sectional moment and cross-sectional moment of inertia

¹Tobita, K; ⁺¹Ohnishi, I; ¹Matsumoto, T; ¹Ohashi, S; ¹Bessho, M; ¹Kaneko M; ¹Matsuyama, J; ¹Nakamura, K
⁺ ¹Department of Orthopaedic Surgery, Faculty of Medicine, University of Tokyo, Tokyo, Japan
ohnishii-dis@h.u-tokyo.ac.jp

INTRODUCTION

Low-intensity pulsed ultrasound stimulation (LIPUS) reportedly enhances restoration of strength at fracture healing sites according to previous experimental studies [1]. However, evaluation of strength by mechanical testing is limited to only one direction, with either bending or torsion. Quantitative micro computed tomography (μ CT) is able to acquire 3-dimensional (3D) histomorphometric data and density distributions of hard tissues, from which strength-related parameters can be calculated to allow strength analysis of the tissue. Strength-related parameters such as cross-sectional moment (CSM) and cross-sectional moment of inertia (CSMI) have been used to evaluate strength of the fracture healing site and reportedly correlate well with measured strength from mechanical testing [2]. However, previous studies have performed 2-dimensional (2D) analyses, and 3D evaluations have not been described. The purpose of this study was thus to investigate the effects of LIPUS on osteotomy healing using conducting 3D analyses of strength-related parameters of CSM and CSMI derived from μ CT of the osteotomy gap.

MATERIALS AND METHODS

Surgical Procedures and LIPUS Treatment

A total of 42 skeletally mature between 21 and 23-week-old male Japanese white rabbits (Kitayama Labes, Nagano, Japan), weighing 3.4-4.0 kg, were used for this study. Under general anesthesia, four transfixation pins (diameter, 2 mm; length, 50 mm) were inserted at the metaphyseal regions of the tibia in the frontal plane using a custom-made surgical pin driver. Transverse osteotomy was performed using a T-saw (blade thickness, 0.36 mm) with continuous irrigation with saline solution across the mid-shaft of the tibia at 12 mm distal to the tibio-fibular junction. The osteotomy with a 2-mm gap was immobilized with four pins fixed to an external fixator with double side bars.

The LIPUS system (model SAFHS[®]2000J, Teijin Pharma, Tokyo, Japan), which transmits 200- μ sec burst of 1-MHz sine waves repeated at 1kHz with an average intensity of 30mW/cm², was used. After postoperative day 3, LIPUS was continued under general anesthesia for both the treatment group (n=7/group/time point) and the control group (n=7/group/time point). The transducer was placed onto the anterior surface of the operated leg with ultrasound coupling gel, for 20 min, six times/week, for 4, 6, or 8 weeks. The control group also received a sham inactive transducer under exactly the same condition as the LIPUS group.

μ CT Analysis

All animals were euthanized and the entire tibia was removed. The harvested tibia was scanned by μ CT system (Scan X mate-E090, Comscantecno, Kanagawa, Japan). The scan was performed along the long axis of the diaphysis, with a voltage of 60 kVp and a current of 80 mA. Scan range covered 5 mm proximal and 5 mm distal to the center of the gap, with a resolution of 28.57 μ m³ voxel size. The region of interest (ROI) was set at the callus healing area (Fig. 1) defined by the gap filled with callus in 2D CT and extended 0.5 mm proximally and distally to the center of the osteotomy gap with a total of 36 CT axial scans. 3D reconstruction of mineralized tissue was performed using a TRI-BONE system (Ratoc System Engineering, Tokyo, Japan). A threshold for newly formed mineralized callus was set as 200 mg/cm³. Morphometric parameters used for evaluation were mineralized callus volume (BV, cm³) and mineralized callus contents (BMC, mg) calculated from the contoured ROI in 3D images, and volumetric bone mineral density of mineralized tissue comprising the callus (mBMD, mBMD = BMC/BV, mgHA/cm³).

Center of gravity for the ROI was calculated automatically. The Z (polar) axis was defined to coincide with the long axis of the tibia. The Y axis was defined as parallel to the transfixation pins, which were also parallel to the posterior surface of the tibia (mediolateral (ML) direction). The X axis was defined as perpendicular to the YZ plane, and was directed anteroposterior (AP) on the tibia (Fig. 2).

Three-dimensional CSM and CSMI

An optional line (I) can be drawn in this XYZ coordinate. The angle of the Z axis (θ) was measured, and also the degree of angle of the X axis (ϕ) was measured (Fig. 3). The 3D CSM [$I(\phi, \theta)$] around this line was calculated as shown. 3D CSM was calculated using the following

equation: $I(\phi, \theta) = \int r^2 dV$ (mm⁵), where r is the distance of a voxel to the center of gravity (mm) and dV (BV/voxel) is the area of a voxel (mm³). The axial CSM was defined as CSMx: $I(0, 90)$, CSMy: $I(90, 90)$, whereas the polar CSM was also defined as CSMp: $I(\text{any}, 0)$. We evaluated these three parameters as bone strength indices.

3D CSMI weighted by density distribution was calculated using the following equation: $I'(\phi, \theta) = \int \rho r^2 dV$ (mgmm²), where r is the distance of a voxel to the center of gravity, dm is the measured mineral content of a voxel in callus (BMC/voxel), ρ is the measured volumetric callus mineral density (mBMD), and dV (BV/voxel) is the area of a voxel (mm³). CSMI x: $I'(0, 90)$, CSMI y: $I'(90, 90)$, and CSMI p: $I'(\text{any}, 0)$ were calculated. These three parameters were evaluated as bone strength indices.

Statistical Analysis

The μ CT evaluations were analyzed using a one-way ANOVA test. Data were all presented in mean and standard deviation (SD). Statistically significant difference was set at $p < 0.05$.

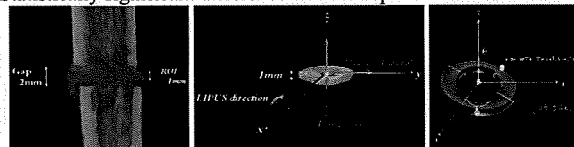


Fig. 1 (left): Region of interest was set at the callus healing area. It defined as a center of the osteotomy gap with a width of 1 mm.

Fig. 2 (middle): The XYZ plane was showed. The LIPUS transducer was placed onto the anterior surface of the operated leg

Fig. 3 (right): An optional line (I) can be drawn in this XYZ coordinate.

RESULTS

Three-dimensional CSM and CSMI

3D CSMs at the same time point were compared, values for the LIPUS groups were significantly higher than those for control groups for CSMx at 6 weeks ($p < 0.05$) and CSMp at 8 weeks ($p < 0.05$), Fig. 4A.

3D CSMIs at the same time point were compared, values for the LIPUS groups were significantly higher than those of the control groups for MOIx, MOIy, and MOIp at 6 and 8 weeks (Fig. 4B).

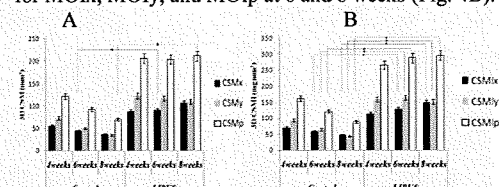


Fig. 4A-B. The result of 3D CSM (left) and 3D CSMI (right) were showed. * = $p < 0.05$.

DISCUSSION

CSM and CSMI are related to architectural strength and show bending and torsion properties. CSMI is a more reliable predictor than CSM for actual bone strength. CSMIp indicates torsional bone property, whereas the axial CSMIs of CSMIx and CSMIy indicate bending properties around the X and Y axes, respectively. We adopted 3D strength-related architectural parameters derived from μ CT scans of the callus to evaluate the effects of LIPUS on restoration of mechanical integrity of the gap healing site.

Our results demonstrate that these bone strength parameters improved with LIPUS during the early phases. However, whether the late phase of callus formation is influenced remains unclear. The present study did not conduct mechanical testing, but μ CT scans evaluated strength-related parameters in three independent planes. Mechanical testing can evaluate strength in only one plane for one specimen. Our results demonstrated that LIPUS improves initial restoration of strength at the healing site in bending in AP and ML planes, as well as torsion.

REFERENCES

1. Pilla AA et al, *J Orthop Trauma*, 1990
2. JL Ferretti et al, *J Musculoskel Neuron Interact*, 2001

ACKNOWLEDGEMENT

This project was supported by Teijin Pharma Limited, Tokyo, Japan.

Evaluation of the Accuracy of Articular Cartilage Thickness Measurement by Conventional and Real-time Spatial Compound Ultrasonography

¹Ohashi, S; +¹Ohnishi, I; ¹Matsumoto, ¹Bessho, T; ¹Matsuyama, J; M; ¹Tobita, K; ¹Kaneko M; ¹Nakamura, K
⁺ Department of Orthopaedic Surgery, Faculty of Medicine, University of Tokyo, Tokyo, Japan
ohnishii-dis@h.u-tokyo.ac.jp

INTRODUCTION

Articular cartilage thickness has previously been quantified by B-mode ultrasonography [1, 2]. However, cartilage surface and cartilage-bone borders have been decided manually in those studies. In addition, no studies have adopted real-time spatial compound ultrasonography for measuring cartilage thickness. The purpose of this study was to develop a method to objectively quantify articular cartilage thickness in vitro using both conventional and real-time spatial compound B-mode ultrasonography and to evaluate the accuracy of measurement.

MATERIALS AND METHODS

Cartilage samples

Knee joints were obtained for a 6-month- and a 3-year-old pig from a slaughterhouse (Tokyo Shibaura Zouki, Tokyo, Japan), as we assumed that thickness could differ between pigs at different ages. Femoral condyle articular cartilage was used in this study, since cartilage size and shape are relatively similar to those of human knee articular cartilage. After slaughter, whole bodies of pigs were kept at 3 °C in a refrigerated room. On the third day, the hind limbs were detached and sent to our laboratory under the same temperature. In our laboratory, limbs with intact knee joints were packed in plastic bags, degassed manually, sealed hermetically and stored at -20 °C. On the day of the experiment, soft tissues including joint capsules and ligaments were removed after the limbs were thawed in normal saline solution (Otsuka Pharmaceutical, Tokyo, Japan) at room temperature. Osteochondral blocks with the surface size of 20 × 20 mm from the medial femoral condyle were acquired by cutting the bone with a band saw (SWD-250; Fujiwara Sangyo, Miki, Japan), then fixed on a custom-made acryl sample holder (30 × 30 × 13 mm; Murai & Co., Tokyo, Japan) with resin (GC-Ostron; GC Corporation, Tokyo, Japan). During preparation, samples were continuously cooled and moistened using normal saline solution.

Acoustic measurement

A B-mode 10.0-M Hz linear ultrasound probe (UST-5411; Aloka, Tokyo, Japan) connected to an ultrasound device (Prosound ALPHA 10; Aloka) was attached to a holding arm, which was fixed to a stage with an x,y micrometer for horizontal adjustment to enable identification of the location of cartilage measurement. In the water tank, osteochondral blocks and the transducer surface were placed in 20 °C water. The distance between transducer surfaces and the sample was kept as the transducer focus distance. Edges of the sample were identified by ultrasound signals, and the center of the sample was then identified from those points. B-mode images of the center line of the sample holder were acquired (Fig. 1A). Image settings were for both conventional imaging and real-time spatial compound imaging superimposed with three frames each from a different viewing angle of -20, 0, and 20 degrees to the right angle. System settings were optimized for imaging the cartilage surface. Brightness line data of 32 points at 0.5-mm intervals in each image were obtained from both the 6-month- and 3-year-old pigs (Fig. 1B). The cartilage surface and cartilage-bone border of the specimen were defined as the peaks of each reflected signal. Cartilage thickness (Tc-US) was measured as the distance between peaks, which was adjusted by the ultrasound speed for each age from our past study [3].

Optical thickness measurement

The specimen fixed to the custom-made sample holder was mounted on a diamond saw device (Minitom; Struers, Westlake, OH), which offers an accuracy of 10 μm for adjustment of the cutting plane. A center-cut plane of the acryl sample holder was created, corresponding to the B-mode ultrasound image plane. Subsequently, each sample was mounted on a glass slide, covered with a cover glass after dripping normal saline onto the sample surface to keep the cartilage moistened and inhibit deformation during measurement due to drying. Cartilage thickness was measured using optical measuring microscopy (MM-400; Nikon, Tokyo, Japan). Using this optical measuring microscopy, points of line data acquisition on the cartilage surface and direction of the US beam were able to be identified from the position and orientation of the acryl sample holder surrounding the cartilage sample. Thickness of the cartilage (Tc) along the beam direction was measured at each point.

Mean and standard deviation (SD) of Tc for each sample were calculated. Linear regression analysis was performed and Pearson's

coefficient of correlation was used to compare Tc-US to Tc. A correlation was considered significant for values of p<0.05.

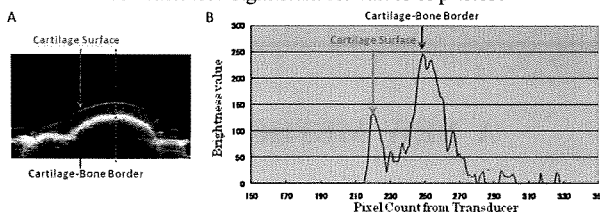


Figure 1: A) B-mode ultrasound image of the sample is shown. B) Line data acquired from the dotted line in the ultrasound image (A). Peak of the reflected ultrasound signal were defined as the surface and border of the tissue.

RESULTS

In all B-mode line data, peaks of reflected ultrasound signals from the cartilage surface and cartilage-bone border were clear enough to be identified. Mean Tc and Tc-US (conventional, spatial compound) for both samples are shown in Table 1. Tc-US was significantly correlated with Tc in both the 3-year- and 6-month-old pigs (p<0.0001 each) (Fig. 2). Pearson's coefficient of correlation tended to be slightly higher with spatial compound in each sample.

	6-month-old pig	3-year-old pig
Tc (mm)	2.40 ± 0.39	1.49 ± 0.10
Tc-US (conventional)	2.46 ± 0.42	1.45 ± 0.18
Tc-US (spatial compound)	2.40 ± 0.47	1.47 ± 0.14

Table 1. Mean Tc and Tc-US (mm). Values are provided as mean ±SD.

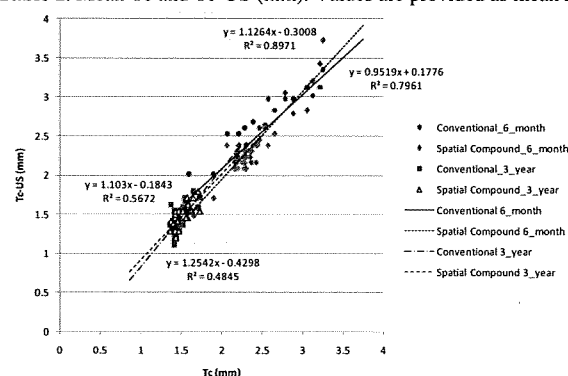


Figure 2. Scatter plot of each ultrasound image setting and sample. Linear regression analysis shows good agreement between Tc and Tc-US in all plots.

DISCUSSION

This is the first study to measure Tc using real-time spatial compound ultrasonography, which has been adopted in evaluating other tissues, such as tendon [4] and ligament [5]. From our results, real-time spatial compound ultrasonography may potentially have higher accuracy for measuring Tc than conventional methods, even though both showed good accuracy in our study. We believe the accuracy of our method is sufficiently high to allow application to measure human Tc in future studies.

REFERENCES:

- [1] Myers et al. J Rheumatology, 1995; 22; 109-16.
- [2] Burkhard et al. Arthritis & Rheumatism, 2009; 61; 435-41.
- [3] Ohashi et al. 55th Orthopaedic Research Society, 2009.
- [4] Bartolotta et al. Radiol Med. 2007 ; 112 ; 562-71.
- [5] Sorrentino et al. Radiol Med. 2009 ; 114 ; 312-20.

ACKNOWLEDGEMENT:

This work was funded by the grant in aid of the Comprehensive Research on Aging and Health H19-007 of the Health and Labour Sciences Research Grants from the Ministry of Health, Labour and Welfare of Japan.

● *Original Contribution*

A NEW METHOD FOR EVALUATION OF FRACTURE HEALING BY ECHO TRACKING

JUNTARO MATSUYAMA,* ISAO OHNISHI,* RYOICHI SAKAI,† MASAHIKO BESSHO,*
TAKUYA MATSUMOTO,* KOICHI MIYASAKA,† AKIMITSU HARADA,† SATORU OHASHI,*
AND KOZO NAKAMURA*

*Department of Orthopaedic Surgery, University of Tokyo and †Research Laboratory, Aloka Co. Ltd., Tokyo, Japan

Abstract—Assessment of bone healing on radiographs depends on the volume and radio-opacity of callus at the healing site, but is not necessarily objective, and there are differences of judgment among observers. To overcome this disadvantage, a clinical system was developed to quantify the stiffness of healing fractures of the tibia in patients by the echo tracking (ET) method in a manner similar to a three-point bending test. The purpose of this study was to ensure that the ET system could clinically assess the progress, delay or arrest of healing. The fibular head and the lateral malleolus were supported. A 7.5-MHz ultrasound probe was placed on the proximal and distal fragments and a load of 25 N was applied. Five tracking points were set along the long axis of the ultrasound probe at intervals of 10 mm. With a multiple ET system, two probes measured the displacement of five tracking points on each of the proximal and distal fragments of the tibia, thereby detecting the bending of the two fragments generated by the load. ET angle was defined as the sum of the inclinations of the proximal and distal fragments. Eight tibial fractures in seven patients treated by a cast or internal fixation were measured over time. In patients with radiographically normal healing, the bending angle decreased exponentially over time. However, in patients with nonunion, the angle remained the same over time. It was demonstrated that the ET method could be clinically applicable to evaluate fracture healing as a versatile, quantitative and noninvasive technique. (E-mail: ohnishi-dis@h.u-tokyo.ac.jp) © 2008 World Federation for Ultrasound in Medicine & Biology.

Key Words: Ultrasound, Echo tracking, Fracture site stiffness, Fracture healing.

INTRODUCTION

The most important issue in assessment of fracture healing is to obtain information about restoration of the mechanical integrity of the bone. In clinical practice, fracture healing is usually judged from serial radiographs. Assessment of bone healing on radiographs depends on the volume and radio-opacity of callus at the healing site, but is not necessarily objective, and there are differences of judgment among observers. In addition, radiographs cannot evaluate fracture site strength. In these respects, assessment of fracture healing by using radiographs is far from ideal.

The stated disadvantages of radiography for assessment of fracture healing have been pointed out in recent years, and various other methods of assessment have been developed. Jernberger (1970) devised an invasive

method for measuring the bending stiffness of healing fractures of the tibia. With his method, the proximal and distal bone fragments were fixed by screws that were connected to a specially designed beam, and a load was applied through a screw at the center of the fixing screws. The method was based on the principle governing the bending of two beams connected at the ends and subjected to a bending force applied at the midpoint. Burny et al. (1984) developed a method that used a strain gauge attached to a fixator shaft. With their method, the strain gauge readings were monitored over time during weight bearing, and the pattern of fracture healing was classified into seven categories (such as normal, delayed, arrested, etc.). Assessment using acoustic emission (AE) was developed by Nicholls and Berg (1981), who detected acoustic pulses generated by microscopic failure of the bone under loading. The investigation by Watanabe et al. (2001) revealed that AE signals occurred with the yielding of callus. However, the strain gauge method and the AE method have the disadvantage that both are limited to patients with external fixation, and both require the in-

Address correspondence to: Isao Ohnishi, M.D., Ph.D., Department of Orthopaedic Surgery, University of Tokyo, 7-3-1 Hongo, Bunkyo-ku Tokyo, 113-0033, Tokyo, Japan.
E-mail: ohnishi-dis@h.u-tokyo.ac.jp

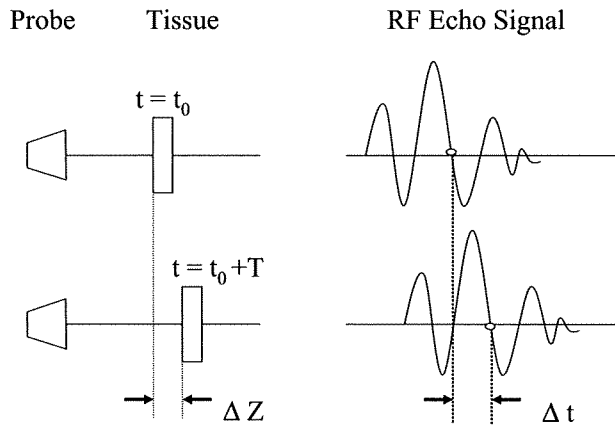


Fig. 1. The target tissue may move closer to or away from an ultrasonic probe over the distance ΔZ during a pulse repetition time of ultrasonic waves (T), causing phase delay of the RF echo signal (Δt). The ET method measures the extent of this displacement by tracking the initialized phase pattern of the echo signal.

sertion of screw pins or wires. For these reasons, such methods have not been widely used and a new method is needed that is both noninvasive and widely applicable.

To overcome such limitations, we developed a new method for the noninvasive and quantitative assessment of fracture healing. Bone always undergoes deformation in response to an applied load. By quantitatively measuring this deformation, it is possible to assess the mechanical properties of bone and thereby estimate the strength of a fracture site. In this study, we attempted to noninvasively assess the bending stiffness of the healing fracture sites after applying a load. To measure bending stiffness, we focused on ultrasound because it is noninvasive. Precise measurement of the displacement of a specific point can be done by the echo tracking (ET) method. This method is a technique for measuring minute displacement of a certain point on a tissue by detecting a wave pattern in the radiofrequency (RF) echo signal reflected from the target tissue (Fig. 1) (Hokanson et al. 1972). To apply this technique for detection of bone deformation, we improved it so that displacement could be measured with an accuracy of $2.6 \mu\text{m}$ (Matsuyama et al. 2006). We also developed a multi-ET system that was able to simultaneously track dynamic movement at multiple points on the bone surface. In our previous study of the three-point bending test using a porcine tibia, the strain gauge readings and the data from the multi-ET system showed an almost perfect linear correlation with the load ($r = 0.998$). These results indicated the possibility of using the echo tracking method to detect bone surface deformation.

The purpose of this study was to determine whether our newly developed ET system could clinically assess the progress, delay or arrest of healing by detecting the

bending stiffness at the fracture healing site. Fracture healing was evaluated in patients with tibia fracture treated by a cast or internal fixation.

METHODS

A clinical system was developed to quantify the stiffness of healing fractures of the tibia in patients by the ET method in a similar manner to a three-point bending test. Five tracking points were set along the long axis of the ultrasound probe at intervals of 10 mm. With a multiple ET system, two probes measured the displacement of five tracking points on each of the proximal and distal fragments of the tibia, thereby detecting the bending of the two fragments generated by the load. ET angle was defined as the sum of the inclinations of the proximal and distal fragments (Fig. 2). When callus was weak in the initial stage of healing, the tracked points were almost in a straight line and the inclination of the two fragments was calculated directly. However, when the callus was more rigid in the late stage of healing, the line connecting the points was curved and the inclination was obtained from the slope of the linear regression equation for the displacement of the points.

Before clinical application of this method, its accuracy was evaluated by measuring the inclination of the metal flat panel.

Measurement of the accuracy of ET angle using an inclined flat metal panel

A flat stainless steel (SUS 420J) panel (length 270 mm, width 60 mm, thickness 5 mm) was used, which had a parallel accuracy and flatness variation of $<2 \mu\text{m}$. One end of the panel was attached to a magnet stand (DG, Noga Japan Ltd, Saitama, Japan), and the other side was attached to a goniometer (X13-001, Tsukumo Co. Ltd, Saitama, Japan) fixed to another magnet stand. Then, the

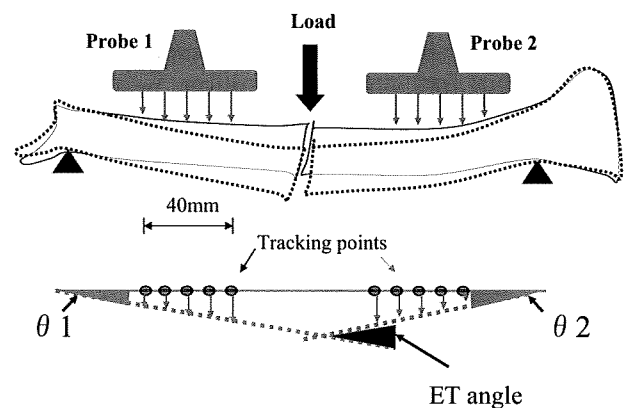


Fig. 2. Probes are set on each of the proximal and distal fragments of the tibia to detect the bending of the two fragments generated by a load. The ET angle is defined as the sum of the inclination of both fragments.

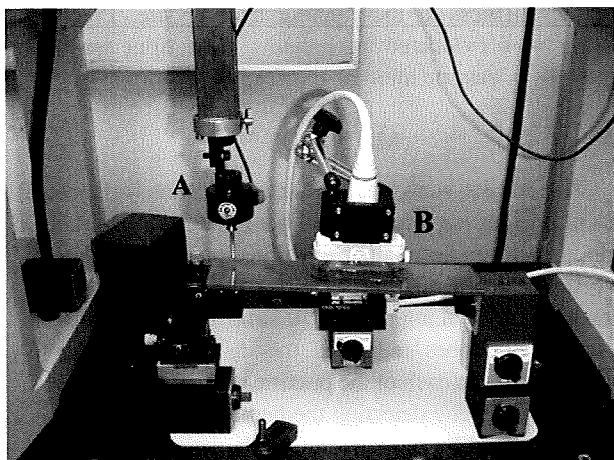


Fig. 3. The accuracy of the ET measurement was evaluated by measuring the inclination of the flat metal panel simultaneously using a 3-D measuring device. (A) 3-D measuring device; (B) 7.5-M Hz linear ultrasound probe.

metal panel was inclined by increasing the height of the goniometer stand. A 7.5-M Hz linear ultrasound probe (UST-5710-7.5, Aloka Co. Ltd., Tokyo) was set at a distance of 20 mm from the panel to measure the changes of displacement of each of five points on the panel (Fig. 3). Using these data, the ET angle of the panel was calculated. At the same time, the inclination of the panel was accurately measured using a 3-D measuring device (AE112, Mitsutoyo, Kanagawa, Japan) with an accuracy of $1 \mu\text{m}$. The panel was inclined by elevating the sliding mechanism of the stand by 0.4 mm and the inclination of the panel was measured 5 times, after which the mean and standard deviation were calculated. Accuracy was evaluated by calculating the standard deviation of the difference between the ET angle and the inclination measured by the 3-D measuring device in each of the measurement trials.

Clinical measurement of fracture site bending stiffness

Eight tibial fractures in seven patients with an average age of 37 y (range 24–69 y) were measured (Table

1). Two fractures of two patients were treated conservatively with a cast, and six fractures of five patients were treated by internal fixation (locked intramedullary nailing in 4, plating in 1 and screws in 1). The average measurement period was 40.8 wk (21–60 wk), and the average number of measurements was 7.5 (5–11).

Patients assumed the supine position with both knees extended, and the affected leg was held horizontal with the antero-medial aspect of the tibia upwards. The fibular head and the lateral malleolus were supported and held tight by a Vacufix (Muranaka Medical Instrument Co., Ltd., Osaka, Japan) to avoid rotation of the leg during loading trials. Before measurement, B-mode images of the short axis of the proximal and distal fragments of the tibia were obtained to identify the center in both directions. By connecting both of the centers, the anatomical axis of the tibia was identified. A 7.5-MHz ultrasound probe was placed on the antero-medial aspect of each of the proximal and distal fragments in the long axis. Each probe was equipped with a multi-ET system with five tracking points at 10-mm intervals. The probes were set vertically on the skin of the leg and held tight with an articulated holder (DG61003, Noga Japan Ltd., Saitama, Japan). A load of 25 N was applied at a rate of 5 N/s and then reduced to 0 N at the same rate using a force gauge (DNP, Imada, Osaka, Japan) parallel to the direction of the probe at the most distal part of the proximal fragment adjacent to the fracture site (Fig. 4). For the initial measurement obtained in each patient, the loading point was set right on the long axis near the fracture site using a B-mode image as a guide. With this setup, the tibia was bent in the same way as for a three-point bending test in the direction of the ultrasound beam. In patients with oblique or spiral fractures, the loading point and the tracking points were set so that they did not cover the fracture site. In patients with a bone graft at the fracture site, the loading point was set on the graft, but the probes were placed so as not to cover it. In the patient with a plate, both the proximal and distal probes were set on the plate surface to measure bending of the plate. Using the multi-ET system, the probes

Table 1. Clinical cases of the tibial fracture

Case	Gender	Age	Limb	Treatment fracture healing	Measurement period (Initial-final)	Radiographic finding
1	F	24	L	Casting	4–47 wk	Normal
2	M	29	R	Casting	7–28 wk	Normal
3	M	23	R	Bone grafting	8–27 mo	Normal
4	M	31	R	Nailing	4–39 wk	Normal
5	F	57	R	Nailing	5–10 mo	Normal
6	F	57	L	Nailing	6–10 mo	Normal
7	F	26	R	Nailing	5 y 2 mo–5 y 7 mo	Nonunion
8	M	69	R	Plating	9–45 wk	Delayed

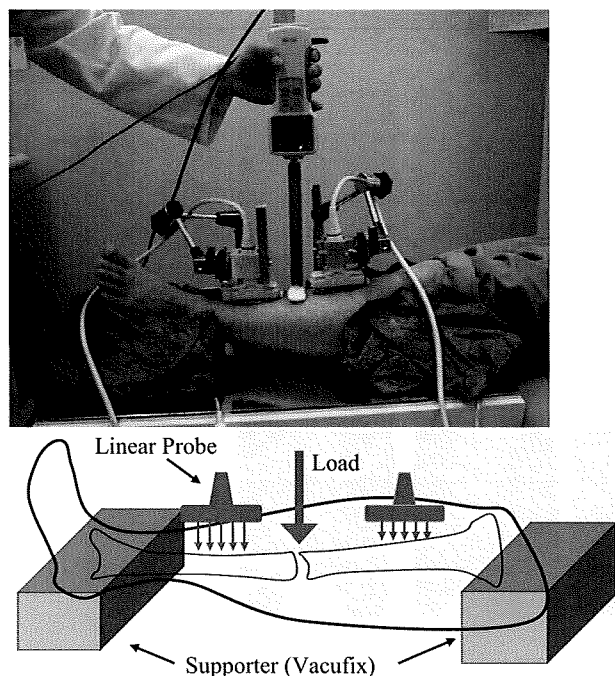


Fig. 4. The affected leg of a patient was held horizontal with the antero-medial aspect of the tibia upwards. The fibular head and the lateral malleolus were supported and held tight by a Vacufix. The probes were set vertically on the skin of the leg and held tight with an articulated arm. A load was applied using a force gauge parallel to the direction of the probe.

detected the angle between the proximal and distal fragments generated by the load. Measurement was repeated five times, and the mean and the standard deviation of the ET angle were calculated.

Fracture healing was assessed at intervals of two or three weeks until radiographic union or arrest of healing occurred. In each patient, the decrease of the ET angle was statistically examined to determine whether it decreased exponentially and whether the decrease was significant. To evaluate the changes of the ET angle over time, exponential regression analysis was performed, and the curve of the ET angle vs. time relation was drawn. Differences were considered significant when the p value was less than 0.05.

To investigate the influence of the position of the probes and the patient on the results, the precision of the method was evaluated by repeated measurement of the ET angle in a patient with a diaphyseal fracture of the tibia treated by a cast (case 2). In addition, the linearity of the relation between the load and the ET angle was assessed by incrementally increasing the load from 10 to 30 N. The ultrasound device (SSD 1000, Aloka Co. Ltd.) used in this investigation is used clinically and its safety has been established. The protocol of this investigation was approved by the ethics committee of The University of Tokyo Hospital, and the patients were enrolled after informed consent was obtained.

RESULTS

Accuracy of ET angle measurement for a flat metal panel

Measurement of the inclination of the flat metal panel showed that the average inclination was 0.117° and the standard deviation was 0.002° . The average inclination obtained with the 3-D measuring device was 0.116° , with a standard deviation of 0.003° . The standard deviation of the differences between the data obtained by the ET method and by the 3-D measuring device was 0.002° .

Clinical measurement of fracture site bending stiffness

The average time required for measurement was 17 min (range 15–20 min). At each loading trial, none of the patients complained of pain and there were no complications related to measurement.

The precision of this method was evaluated by repeating measurement of case 2 (treated with a cast), with repositioning of the leg and the ultrasound probes. The mean and standard deviation of the ET angle were 0.316 ± 0.015 , and the coefficient of variation was calculated to be 4.6%. The linearity of the relation between the load and the bending angle was very high, with a correlation coefficient of 0.997.

Cases presentation

Case 1: A 24-year-old-woman treated with a cast. The patient sustained a spiral fracture of the proximal diaphysis of the tibia in a traffic accident, and a patella tendon bearing brace cast was applied. Healing was assessed by the ET method, as well as radiographs a total of 11 times from 4 weeks to 47 weeks after fracture. The fracture line became opaque and the callus volume increased from 4 weeks to 19 weeks, but after 26 weeks there was almost no change of the thickness of the callus. On the other hand, measurement showed that the ET angle was about 1° at 4 weeks, and that it decreased exponentially ($y = 1.40e^{-0.105x}$, $r = -0.975$, $p < 0.0001$). The ET angles of both cases 1 and 2 treated with a cast decreased exponentially over time and they reached the level of the intact side by 22 weeks (Fig. 5a, b).

Case 7: A 26-year-old-woman with a fracture of the diaphysis of the tibia treated by a locked intramedullary nailing. ET measurement was performed five times from 5 y 2 mo to 6 y 7 mo after fracture. Her X-ray films showed hypertrophic nonunion, but judgment whether healing was proceeding was extremely difficult. ET measurement showed that there was no significant decrease of the angle over a period of 1 y and 5 mo ($y = 0.264e^{0.002x}$, $r = 0.238$, $p = 0.700$) (Fig. 6a, b).

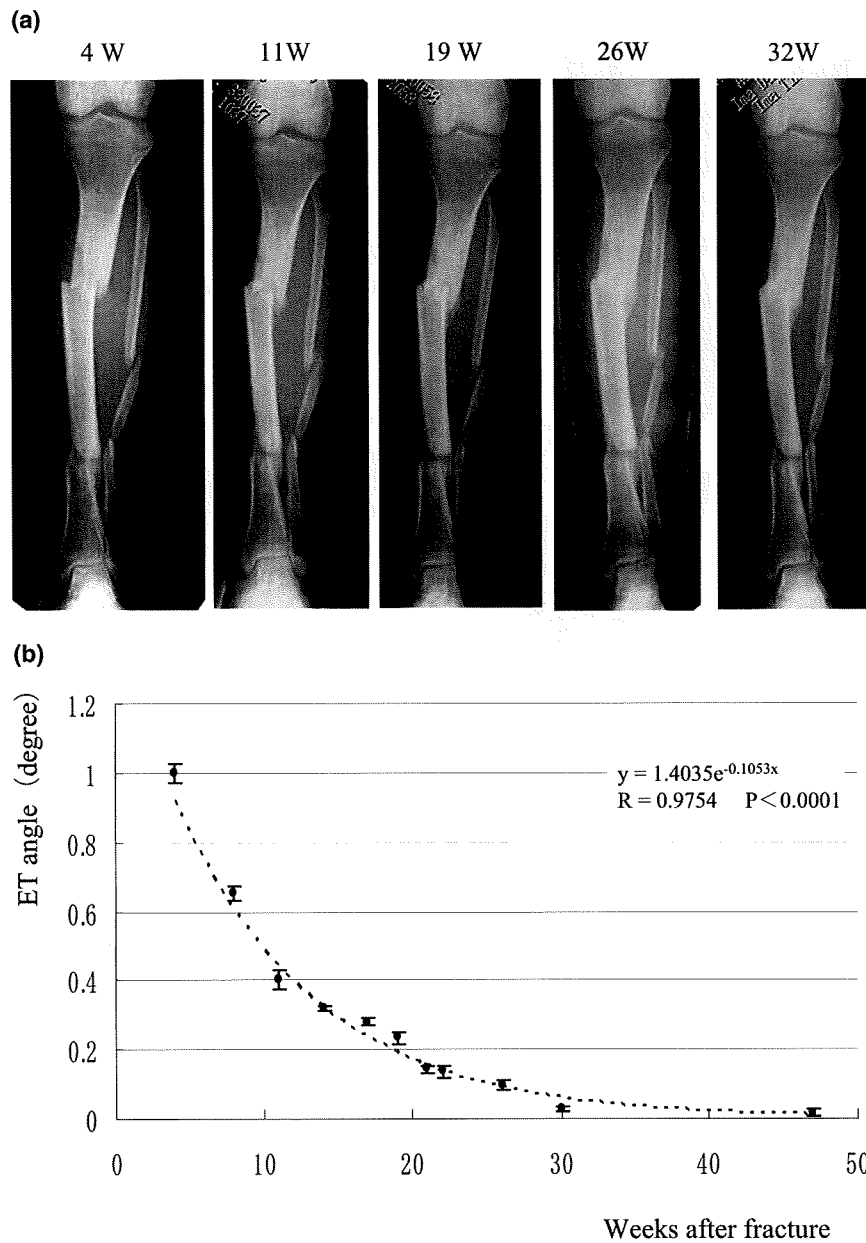


Fig. 5. (a) Time sequential change of the fracture site X-ray from 4 weeks to 32 weeks after fracture in case 1 treated with casting. The fracture site healed normally. (b) In the same patient, the ET angle was plotted. The ET angles decreased exponentially over time.

Case 8: A 69-year-old-man with a long oblique fracture treated with a plate. His X-ray films showed a long oblique fracture line extending for almost 80 mm. Measurement was performed 10 times from 9 weeks to 45 weeks after fracture, during which period almost no change of the fracture site or callus was recognized on X-ray films. The ET method measured the bending angle of the plate. The change was very slow, but the angle decreased significantly from 0.28 to 0.2 degrees, and then finally declined to 0.1 degree. The overall

change showed an exponential curve ($y = 0.40e^{-0.030x}$, $r = -0.895$, $p = 0.0005$) (Fig. 7a, b). In patients with radiographically normal healing, the bending angle decreased exponentially over time (Fig. 8). However, in patients with nonunion, the angle remained the same over time.

DISCUSSION

Our method allows noninvasive assessment of bending stiffness at the healing site, so it can be appli-

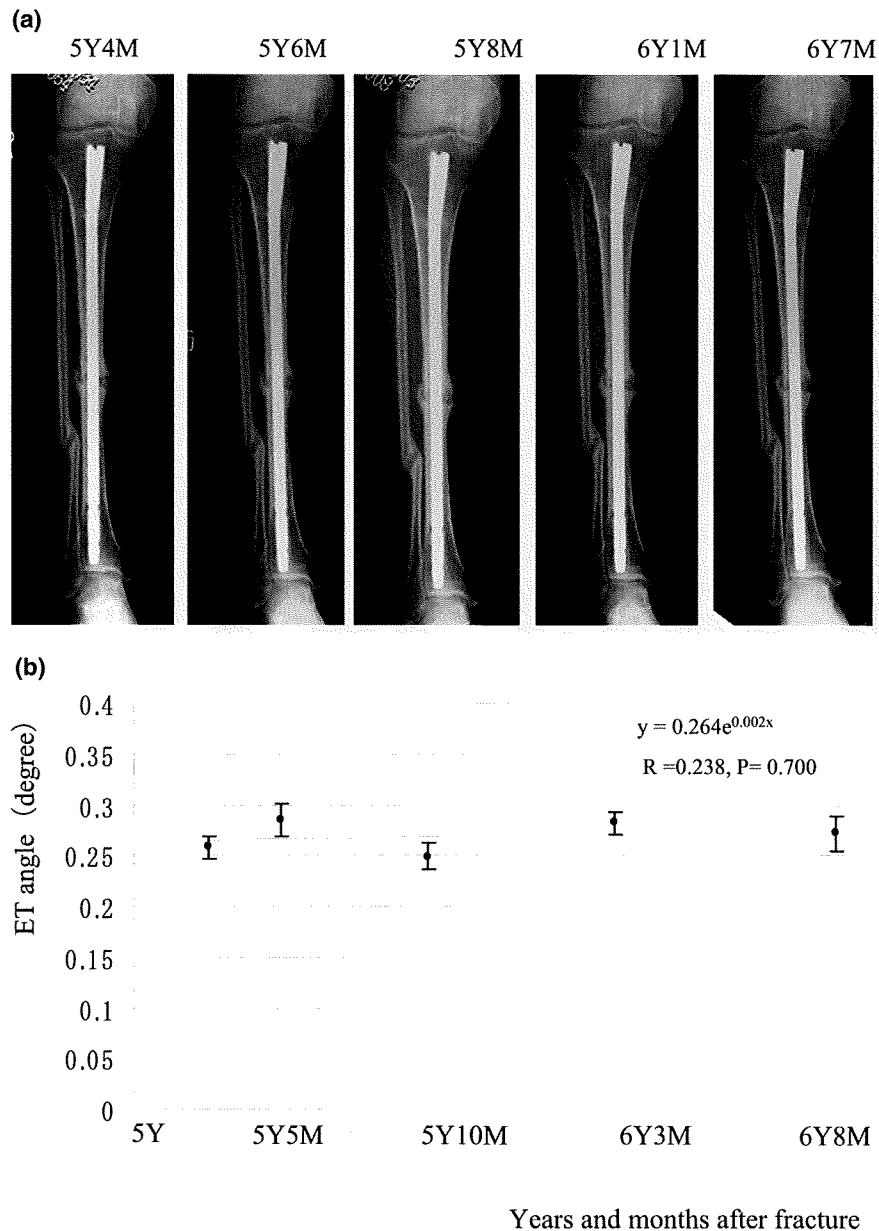


Fig. 6. (a) Time sequential change of the fracture site X-ray from 5 y 4 mo to 6 y 7 mo after fracture in case 7, treated with intramedullary nailing. The X-ray films showed hypertrophic nonunion, but judgment of whether healing was proceeding was extremely difficult. (b) In case 7, the ET angle showed no change over time and the regression lines showed no significant decrease.

cable to patients treated conservatively as well as those managed by surgical intervention with plating or intramedullary nailing.

In this study, the precision and reproducibility of the method were evaluated. The precision of measuring displacement by using the echo tracking system specially designed for bone surface measurement has already been assessed, and a precision of 2.6μ was demonstrated in our previous study. However, the precision of measuring the bending angle has not been investigated before. We

obtained a precision of 0.002° , which was thought to be adequate based on the results of the study by Moorcroft et al. (2001) that evaluated fracture healing. They used the three-point bending test to generate angles of 0.4 to 1.0° in an *in-vivo* measurement trial and connected a goniometer to the bone fragment *via* screw pins fixed to a side bar of the external fixator to detect bending at the fracture site.

When estimation of the linearity of measurement was done in relation to the load, there was excellent

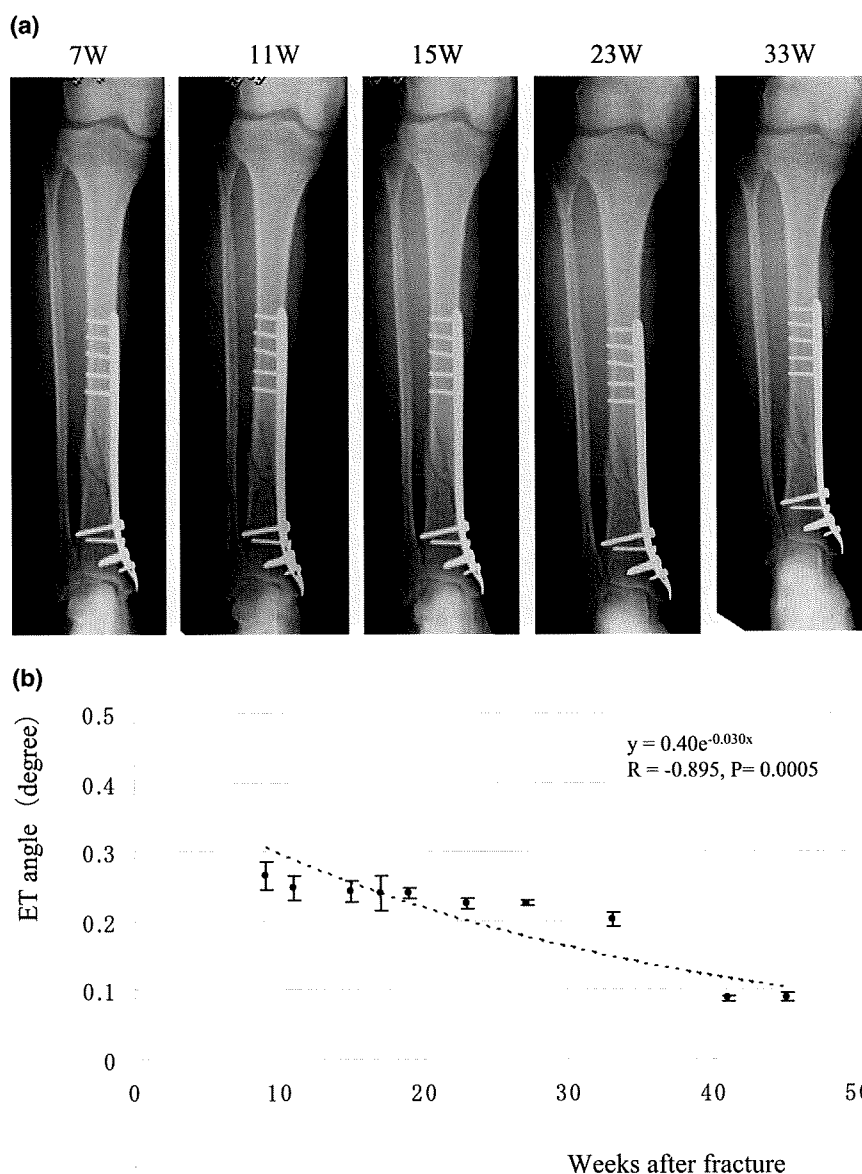


Fig. 7. (a) The X-ray films of case 8, treated with plating. No change of the fracture site or callus was recognized on X-ray films. (b) The ET method measured the bending angle of the plate. The change was very slow, but the angle decreased significantly from 0.28 to 0.2°, and then finally declined to 0.1°.

linearity between magnitude of the load and the ET angle ($r = 0.997$), indicating that elastic deformation of the fracture site had occurred under a load range of 10 to 30 N. Therefore, measurement was shown to be noninvasive as well as safe, without causing any residual deformity.

Reproducibility of the measurement method was estimated to be 0.015° , which was adequate to evaluate fracture healing quantitatively, because the angle ranged from around 1° in the initial stage to about 0.1° in the final stage when it was almost equivalent to that of the intact tibia. However, we have to improve the reproducibility of measurement *in vivo*. The factors affecting reproducibility *in*

in vivo include the position of the leg, loading direction and positions of the probes. Among these, the positioning or fixation of the leg seems to have the most influence on the reproducibility of measurement.

For clinical evaluation of fracture healing, data obtained by the ET method were compared with X-ray findings over time. In patients with delayed healing or nonunion, judgment of the healing process using X-ray films was difficult because the direction and conditions of obtaining images were not exactly the same every time, so the findings were not reproducible. In contrast, the echo tracking method evaluated fracture stiffness

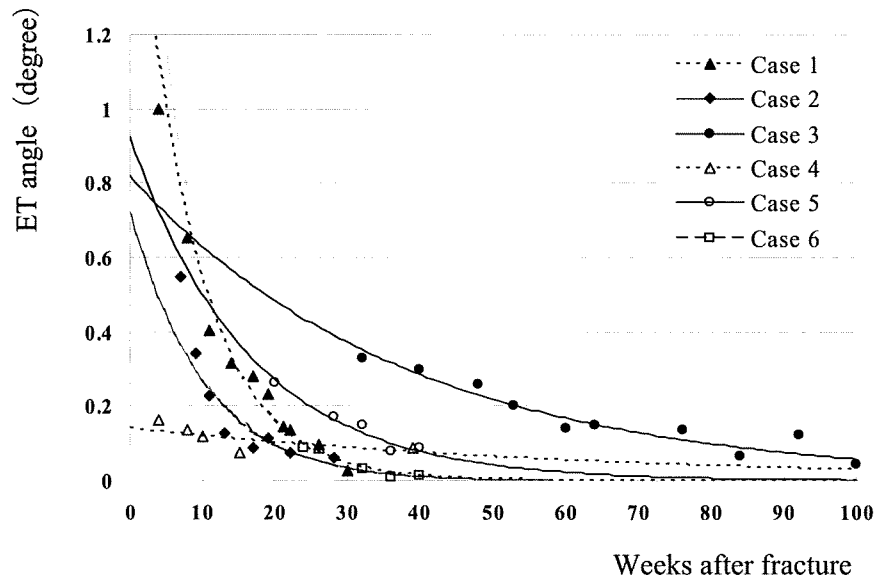


Fig. 8. In cases 1 through 6, the changes of the ET angle showed an exponential pattern. The correlation coefficients obtained by the regression equation for the ET angle and time were very high in these cases.

with considerable accuracy, sensitivity and reproducibility.

In patients with radiographically normal healing, the bending angle decreased exponentially over time. However, in patients with nonunion, the angle remained the same over time. According to the results obtained with previous methods such as the strain gauge method and the invasive method of Jernberger (1970), strain or deformation caused by loading at the healing site has been reported to diminish exponentially over time in patients with normal healing. Among these previous studies, Bourgois and Burny (1972) evaluated fracture healing in hundreds of patients treated with an external fixator that was instrumented with a strain gauge. They not only accumulated considerable clinical data on the strain readings over time, but also theoretically proved by mathematical simulation that the change of the strain over time during normal healing could be expressed as a typical hyperbolic curve. In addition to this, they proved that the time course of the change in strain could also be a hyperbolic curve by developing fracture simulation models with stabilization by intramedullary nailing, plating and external fixation. As a result, their clinical data were compatible with those for the theoretical model of external fixation. They classified the pattern of fracture healing into seven categories depending on the difference in the healing process. Among them, normal healing was defined as healing in which the strain reading vs. time curve reaches a plateau at 60 to 90 days after fracture. Slow healing was defined as healing in which the decline of strain was very slow compared with the

normal pattern but the healing process was progressive over time. Nonunion was defined as cessation of the progress of healing. In two patients treated with a cast in our study, the ET angle decreased rapidly until 10 weeks after fracture to a level twice that on the intact side, and then it decreased slowly. The exponential regression curve for the echo tracking angle vs. time showed a very strong correlation (case 1, $r = -0.975$). Therefore, it can be concluded that the echo tracking method could be used to evaluate normal healing as proposed by Burny et al. (1984). As shown in Fig. 5, the progress of healing in patients treated with intramedullary nailing and bone grafting could be assessed by using the ET method. The ET angle vs. time relation in these cases was also expressed by exponential curves. However, the ET angle curve of patient 7 (Fig. 6b) did not show any significant decrease of the angle and there was no correlation between the ET angle and time. From this, the healing process was diagnosed as nonunion. The ET angle of patient 8, treated with plating, showed an extremely slow decrease over time from 9 weeks to 33 weeks, but reduction of the angle was statistically significant until 45 weeks, so the healing process was concluded to be delayed.

Fracture site stiffness was adopted as a parameter for evaluation that was thought to be correlated with strength of bone healing. In various earlier studies of fracture site mechanical properties, stiffness was measured to estimate the strength of the fracture site. However, stiffness is not necessarily correlated with strength. Chegade et al. (1997) investigated this relationship in 24

sheep. The tibia was stabilized with an external fixator and then osteotomy was done. Next, the tibiae were excised at 6, 8 and 10 wk after osteotomy and a 4-point bending test was done. As a result, in the initial stage of healing, stiffness showed a strong correlation with strength ($r = 0.89$), but there was no correlation between them in the remodeling stage. However, as Chehade *et al.* (1997) stated, because the stiffness of the fracture site is strongly correlated with the strength until remodeling is initiated, it is clinically significant to monitor fracture site stiffness as a substitute for strength to determine the appropriate level of weight bearing so that patients can avoid refracture because of overloading the fracture site during postoperative management. In the remodeling stage, we need to pay special attention to the relationship between stiffness and strength, even if stiffness reached the same value as the intact side.

Fracture healing was evaluated quantitatively by the echo tracking method in patients treated conservatively as well as by internal fixation. All previous methods of assessment could only be applied to patients treated with an external fixator that required the insertion of wires or screw pins, and none of the methods could achieve evaluation in a totally noninvasive manner. The potential problem with evaluating patients treated with internal osteosynthetic devices such as intramedullary nails or plates is that the stiffness at the fracture site is the sum of stiffness for both the healing fracture and the implant. The stiffness of the implant is very high compared with that of the healing fracture because it is made of a metal such as stainless steel or titanium-aluminum-vanadium alloy. Therefore, the combined stiffness at the fracture site is usually very high compared with that in patients receiving conservative treatment by casting. In such patients with internal osteosynthetic devices, comparison of stiffness with the intact side does not have any meaning

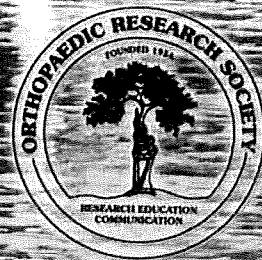
for evaluation of fracture healing. Therefore, we have to be careful with interpretation of the changes of stiffness over time in such cases. How the implanted material and the configuration of stabilization affect fracture site stiffness should be investigated in the future so that we can assess fracture healing more precisely in patients with internal fixation.

In conclusion, it was demonstrated that the echo tracking method could be clinically applicable to evaluate fracture healing as a versatile, quantitative and non-invasive technique. Further development of this method should be performed so that it can be applied to other anatomical sites by improving accuracy and precision.

Acknowledgements—This work was funded in part by a grant from the Pharmaceutical and Medical Devices Agency of Japan.

REFERENCES

- Bourgeois R, Burny F. Measurement of the stiffness of fracture callus in vivo. A theoretical study. *J Biomech* 1972;5:85–91.
- Burny F, Donkerwolcke M, Bourgeois R, Domb M, Saric O. Twenty years experience in fracture healing measurement with strain gauges. *Orthopedics* 1984;7(12):1823–1826.
- Chehade MJ, Pohl AP, Pearcy MJ, Nawana N. Clinical implications of stiffness and strength changes in fracture healing. *J Bone Joint Surg [Br]* 1997;79-B:9–12.
- Hokanson DE, Mozersky DJ, Sumner DS, Strandness DEJ. A phase-locked echo tracking system for recording arterial diameter changes in vivo. *J Appl Physiol* 1972;32(5):728–733.
- Jernberger A. Measurement of stability of tibial fractures. A mechanical method. *Acta Orthop Scand* 1970;135(suppl):1–88.
- Matsuyama J, Ohnishi I, Sakai R, Suzuki H, Harada A, Bessho M, Matsumoto T, Nakamura K. A new method for measurement of bone deformation by echo tracking. *Med Eng Phys* 2006;28(6):588–595.
- Moorcroft CI, Ogrodnik PJ, Thomas PBM, Wade RH. Mechanical properties of callus in human tibial fractures: A preliminary investigation. *Clin Biomech* 2001;16:776–782.
- Nicholls PJ, Berg E. Acoustic emission properties of callus. *Med Biol Eng Comput* 1981;19(4):416–418.
- Watanabe Y, Minami G, Takeshita H, Fujii T, Takai S, Hirasawa Y. Prediction of mechanical properties of healing fractures using acoustic emission. *J Orthop Res* 2001;19(4):548–553.



55th Annual Meeting of the Orthopaedic Research Society

Program Book

The Venetian Hotel • Resort • Casino/
Sands Expo Convention Center
Las Vegas, Nevada
February 22 – 25, 2009

THE
VENETIAN®
THE PALAZZO®

Evaluation of Measurement Precision for Articular Cartilage Ultrasound Speed by Time of Flight Method

¹Ohashi, S; ⁺Ohnishi, I; ¹Matsumoto, T; ¹Matsuyama, J; ¹Bessho, M; ¹Tobita, K; ¹Kaneko M; ¹Nakamura, K

⁺ Department of Orthopaedic Surgery, Faculty of Medicine, University of Tokyo, Tokyo, Japan
ohnishii-dis@h.u-tokyo.ac.jp

INTRODUCTION:

Ultrasound speed in articular cartilage needs to be determined for morphological evaluation of cartilage using ultrasonography. However, relatively variant values of speed (1658 m/s [1], 1892 m/s [2], ca. 1580 m/s [3]) have been reported in past studies on ultrasound speed in human articular cartilage. Although such variability in speed may originate from error of the measurement method [4] and individual speed differences in samples, no studies have clarified the precision of the measurement method. The purpose of this study was to develop a method of measuring cartilage ultrasound speed and to evaluate the precision of our original measurement method.

MATERIALS AND METHODS:

Cartilage samples

Knee joints of a 6-month-old pig and a 3-year-old pig were obtained from a slaughterhouse (Tokyo Shibaura Zouki, Tokyo, Japan), since we assumed the speed could differ between pigs at different ages. Swine femoral condyle articular cartilage was used in this study, since cartilage size and shape are relatively similar to human cartilage. After slaughter, whole bodies of pigs were kept at 3 °C in a refrigerating room. On the third day, the hind limbs were detached and sent to our facility under the same temperature. In our facility, the limbs with intact knee joints were packed in plastic bags, degassed manually, sealed hermetically and stored at -20 °C. On the day of the experiment, soft tissues including joint capsules and ligaments were removed after the limbs were thawed in normal saline solution (Otsuka Pharmaceutical, Tokyo, Japan) at room temperature. Osteochondral blocks from the medial femoral condyle were acquired by cutting the bone with a band saw (SWD-250; Fujiwara Sangyo, Miki, Japan), then fixed on a custom-made acryl sample holder (30 x 30 x 13 mm; Murai & Co., Tokyo, Japan) with resin (GC-Ostron; GC Corporation, Tokyo, Japan). During preparation, samples were continuously cooled and moistened using normal saline solution. The osteochondral block was then trimmed using a diamond saw (Minitom; Struers, Westlake, OH) to achieve a sample cartilage surface size of 10 mm x 10 mm.

Acoustic measurement

A radiofrequency (RF) signal-acquiring system equipped with a 10.0-MHz pulse-echo transducer (diameter, 13 mm; radius of curvature, 60 mm; model V311-SU; Olympus NDT, Waltham, MA) connected to a pulser/receiver (NDT-5800; Olympus NDT) was used for measurements. The transducer and sample holder were attached to a custom holding assembly, which has a sample stage with x, y and θxy micrometer adjustment to enable identification of the location of cartilage measurement (Fig. 1A). In the water tank on the stage, osteochondral blocks and the transducer surface were placed in 20 °C water. The distance between transducer surfaces and the sample was kept as the transducer focus distance. RF signals were recorded using an oscilloscope (DPO4034; Tektronix Japan, Tokyo, Japan). Edges of the sample were identified by RF signals, then the center of the sample was identified from those points. RF signals of 9 points at 1-mm intervals at the center of the sample were obtained from both the 6-month-old and 3-year-old pigs (Fig. 1B). Sampling time was 0.2 ns. A bandpass filter (1.0-20.0 MHz) was used to enhance ultrasound signal-to-noise ratio. TOF was defined as the duration (Δt) between peaks of RF signal envelope, corresponding to the travel time of the US pulse back and forth between the cartilage surface and cartilage-bone border of the specimen (Fig. 2).

Optical thickness measurement

The specimen fixed to a custom sample holder was mounted on the diamond saw device (Minitom; Struers), which has an accuracy of 10 μm for adjustment of the cutting plane. Three cut planes were created, each containing 3 RF signal acquisition points. Subsequently, each 1-mm slice sample was mounted on a glass slide, covered with a cover glass after dripping normal saline onto the sample surface to keep the cartilage moistened and inhibit deformation due to drying during measurement. Cartilage thickness was measured using optical measuring microscopy (MM-400; Nikon, Tokyo, Japan). Using this optical measuring microscopy, the points of RF acquisition on the cartilage surface and direction of the US beam were able to be identified from the position and orientation of the acryl sample holder surrounding the cartilage sample.

Thickness of the cartilage (Tc) along the beam direction was measured at each point and ultrasound speed in cartilage (USc) at each point was calculated: $USc = (2 \times Tc) / \Delta t$

Mean and standard deviation (SD) of each sample were calculated. Student's t-test was used to compare ultrasound speed values between the young and adult pigs. Results were considered significant for values of p<0.05. In addition, the coefficient of variance (CV) for precision evaluation of this ultrasound speed measurement was calculated for each sample.

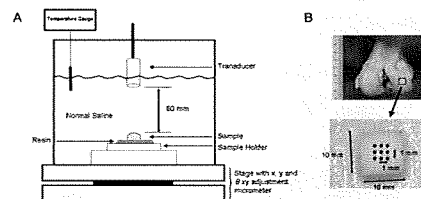


Figure 1A-B. (A) Schematic shows the custom holding assembly. (B) Images show the locations of RF signal acquisition of articular cartilage.

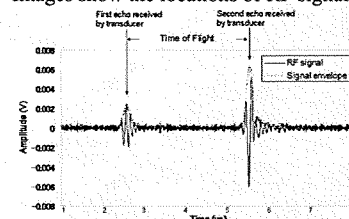


Figure 2. The envelope of the RF signal was calculated and peaks of the envelope were considered as reflection waves of the cartilage surface and cartilage-bone border [3].

RESULTS:

In all RF signals at the 9 points, peaks of reflected ultrasound waves from the cartilage surface and cartilage-bone border were clear enough to be identified. Mean TOF, Tc, USc and CV for both samples are shown in Table 1. With Student's t-test, USc was significantly higher for the 3-year-old pig than for the 6-month-old pig (p<0.0001).

	6-month-old pig	3-year-old pig
Time of Flight (us)	3.455	1.355
Thickness (mm)	2.567	1.161
Ultrasound Speed (m/s) *	1488 ± 48	1717 ± 104
Coefficient of variance (%)	3.1	5.5

Table 1. * Values are described as the mean ± standard deviation.

DISCUSSION:

Several factors are likely to influence the precision of ultrasound speed measurement. First, having sharp peaks of RF signals from the cartilage and cartilage-bone border is very important. For this point, transmitter ultrasound waves must hit the sample surface or border as perpendicularly as possible [4]. The cartilage surface must also be as close as possible to the transducer focus. We focused on measuring TOF with these conditions in our study under our original setting. Second, position adjustment of points between RF signal acquisition and optical thickness measurement is important. We developed a customized assembly in a water tank with the adjustment stage for RF signal acquisition and used a cutting device with very accurate plane adjustment. In addition, the customized acryl sample holder that enabled us to detect the direction of the ultrasound beam in microscopic measurement could achieve registration between ultrasound beam direction and microscopic measurement direction. We believe the precision (3.1 % - 5.5 %) of our method is sufficiently high to allow application to measure the ultrasound speed of human cartilage in future studies.

REFERENCES:

1. Myers et al, J Rheumatol, 22, 1995; 2. Yao et al, Rheumatology, 38, 1999; 3. Nieminen et al, Biorheology, 43, 2006; 4. Mann et al, Rheumatology, 40, 2001;

ACKNOWLEDGEMENT:

This work was funded by the grant in aid of Ministry of Health, Labour and Welfare of Japan.

第82巻

第8号

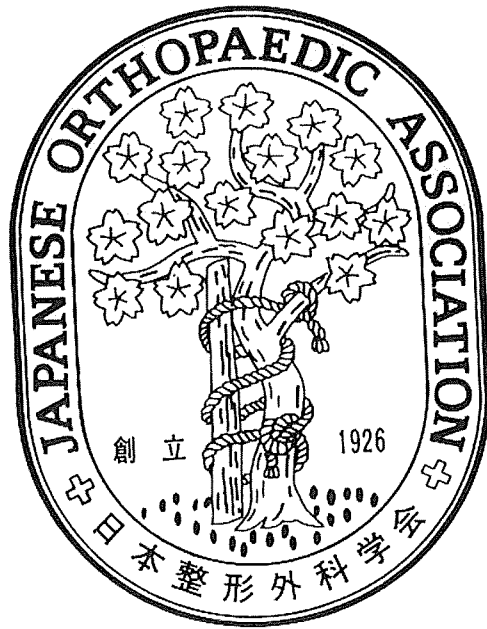
日本整形外科学會雜誌

NIPPON SEIKEIGEKAGAKKAI ZASSHI

The Journal of
the Japanese Orthopaedic Association

Vol. 82 No. 8 August 2008

Proceedings of the 23rd Annual Research Meeting
of the Japanese Orthopaedic Association



日整会誌

日本整形外科学会

J. Jpn. Orthop. Assoc.

1-3-PD1-3

3D-CT (multiplanar reconstruction) による骨癒合の診断および経時的变化の分析

佐藤 徹 堀田 直史 荒瀬 慎也 佐伯 光崇
香川 洋平

【目的】骨折治療の目的は機能障害を残さず骨癒合を得ることであるが、近年の学会報告症例を見て果たして真の骨癒合が得られているのかはなほ疑問な症例も散見する。今回われわれは MPR (multiplanar reconstruction) を用いて、大腿骨近位部骨折の経時的变化について分析し、単純 X 線および臨床評価と対比検討をした。また、当科紹介となった観血的治療を行った癒合不全症例についても同様の検討を行った。

【対象および方法】症例は大腿骨近位部不安定型骨折および Garden stage 2 以上の症例について、術後 3 週目より 3 週間ごとに coronal section の MPR と単純 X 線を撮影し、歩行能力や疼痛などの臨床成績とも対比を行った。MPR は原則として 12 週目まで行うが、臨床的および単純 X 線にて明らかに骨癒合が得られていなければ順次追加撮影した。また、他院にて初期治療を受け癒合不全となり当科紹介となった症例について、2 方向の MPR を検討した。

【結果】大腿骨近位部骨折症例において、MPR にて内側皮質骨および外側皮質骨の連続性を認めた症例では、telescoping の進行が停止し、局所の疼痛も訴えた症例はなかった。また癒合不全症例も術後 12 週以降、coronal section および sagittal section MPR において皮質骨の連続性を認めた症例では全荷重あるいは負荷運動に耐えることが可能であった。

【考察】骨折後骨癒合の判断は苦慮することがしばしばであるが MPR は海綿骨の多い骨幹端部、偽関節部に行った骨移植の判定にも有用であり、骨癒合の判断足りえるものと考えられる。

国立病院機構岡山医療センター整形外科

1-3-PD1-4

超音波エコートラッキング法を用いた骨癒合評価

松山 順太郎¹ 大西 五三男² 酒井 亮一³ 別所 雅彦²
大橋 暁² 宮坂 好一³ 飛田 健治² 松本 卓也²
原田 烈光³ 芳賀 信彦³ 中村 耕三²

【目的】骨癒合を評価するにあたり X 線写真による定性的方法は骨の形状や荷重方向といった力学的情報が欠如しており正確とは言えない。骨癒合においては骨の力学強度の回復が重要であり骨の力学特性を評価することにより骨癒合評価が可能と言える。われわれは体内の骨の重を非侵襲に計測可能なエコートラッキング (ET) 法を用いた新たな診断装置を開発した。ET 法は超音波エコー信号の位相変化を測定するもので、荷重負荷に対する動的な骨の微小変形を 2.6 μm の精度で測定可能とした。この装置を用い、骨の力学特性である剛性測定を行い骨癒合評価を行うことを目的とし臨床測定を行った。

【方法】胫骨骨折患者 (保存療法: 2 名 2 肢、手術療法: 12 名 14 肢) を対象とし測定を行った。下腿の近位・遠位を固定し、骨折部近傍において 25 N の曲げ荷重を加え、近位・遠位骨片の傾斜角 (ET 変形角) を測定した。測定は 2-6 週間隔で実施し、測定期間は平均 21.2 週で測定回数は平均 6.1 回であった。ET 変形角の経時変化を健側肢と比較し骨癒合を定量的評価した。

【結果】保存療法・手術療法のいずれの症例においても X 線上、正常な骨癒合が進行した症例では ET 変形角は経時的に指数関数的に減少し、骨癒合を定量的評価可能であった。一方、手術症例で X 線上、仮骨の形態変化を示さない症例の ET 計測では、いずれも経時測定で明らかな減少はなく、骨癒合不全であることが診断可能であった。

【結論】ET 計測により *in vivo* において非侵襲に骨癒合の進行と遷延が定量的診断可能であった。今後、非侵襲に骨強度評価を行う方法として骨折の骨癒合評価だけでなく脆弱性を有する骨に対しても応用可能であると考えられる。

¹東大リハビリテーション部 ²東大整形外科 ³アロカ研究所